

---

# Study on heat integration of supercritical coal-fired power plant with post-combustion CO<sub>2</sub> capture process through process simulation

Xiaoyan Liu<sup>a</sup>, Jian Chen<sup>a,\*</sup>, Xiaobo Luo<sup>b</sup>, Meihong Wang<sup>b,\*</sup>, Hui Meng<sup>b</sup>

<sup>a</sup>State Key Laboratory of Chemical Engineering, Tsinghua University, Beijing 100084, China

<sup>b</sup>Process and Energy Systems Engineering Group, School of Engineering, University of Hull, HU6 7RX, UK

\*Corresponding author 1. Tel: +86 10 62798627; Fax: +86 10 62770304; Email: [cj-dce@tsinghua.edu.cn](mailto:cj-dce@tsinghua.edu.cn)

\*Corresponding author 2. Tel: +44 1482 466688; Fax: +44 1482 466664; Email: [Meihong.Wang@hull.ac.uk](mailto:Meihong.Wang@hull.ac.uk)

## Abstract

Coal-fired power plant (CFPP) is one of the main sources of anthropogenic CO<sub>2</sub> emissions. Capturing CO<sub>2</sub> from CFPP by post-combustion process plays an important role to mitigate CO<sub>2</sub> emissions. However, a significant thermal efficiency drop was observed when integrating CFPP with post-combustion carbon capture (PCC) process due to the steam extraction for capture solvent regeneration. Thus research efforts are required to decrease this energy penalty. In this study, a steady state model for 600 MW<sub>e</sub> supercritical CFPP was developed as a reference case with a low heating value (LHV) based efficiency of 41.6%. A steady state model for MEA-based PCC process was also developed and scaled up to match the capacity of the CFPP. CO<sub>2</sub> compression process was simulated to give an accurate prediction of its electricity consumption and cooling requirement. Different integration cases were set up according to different positions of steam extraction from the CFPP. The results show that the efficiency penalty is 12.29% and 14.9% when steam was extracted at 3.64 bar and at 9.1 bar respectively. Obvious improvements were achieved by utilizing waste heat from CO<sub>2</sub> capture and compression process, taking part of low pressure cylinders out of service, and adding an auxiliary turbine to decompress the extracted steam. The efficiency penalty of the best case decreases to 9.75%. This study indicates that comprehensive heat integrations can significantly improve the overall energy efficiency when the CFPP is integrated with PCC and compression process.

*Keywords:* process simulation; heat integration; supercritical coal-fired power plant; post-combustion CO<sub>2</sub> capture; CO<sub>2</sub> compression.

## 1. Introduction

Greenhouse gases emissions have been on the increase since the start of industrial revolution. CO<sub>2</sub> is the main greenhouse gas accounting for over 60% of total greenhouse gas emissions [1]. The Intergovernmental Panel on Climate Change (IPCC) indicates that CO<sub>2</sub> emissions need to be cut by a minimum of 50% to limit the average global temperature increment to 2°C in 2050 [2]. Carbon capture and storage (CCS) is considered the key technology to mitigate CO<sub>2</sub> emissions from fossil fuel-based power generation.

A great portion of CO<sub>2</sub> emissions is generated from the electricity and heat industry. Coal combustion is

---

41 estimated to be the largest source of electricity and heat generation, particularly in South Africa (93%),  
42 Poland (92%), China (79%), India (69%), and United States (49%) [3, 4]. The majority of existing CFPPs  
43 are based on subcritical steam cycles, however, supercritical CFPPs are rapidly spreading to replace  
44 subcritical CFPPs, with advantages of higher thermal efficiency and lower CO<sub>2</sub> emissions [5, 6]. The  
45 average thermal efficiency of subcritical CFPPs is 35%, while supercritical CFPPs have about 5%pt higher  
46 net efficiency [7]. Supercritical CFPPs would play an important role in global power generation and the  
47 reduction of coal consumption.

48 Monoethanolamine (MEA)-based chemical absorption technology remains the first choice for CFPP due  
49 to its high operational flexibility because it can be easily integrated into both the existing power plants and  
50 new installations [8]. Moreover, this technology is characterized by a relatively high separation selectivity  
51 [9-12], so that it is well-suited for treating low CO<sub>2</sub> partial pressure flue gas from CFPP [13].

52 Previous studies [14-16] indicates that there is a significant energy penalty when CFPP is couple with  
53 PCC process, because of the steam extraction from CFPPs for solvent regeneration. This high energy  
54 penalty constitutes the main barrier of the commercial deployment of CCS technology. There are two  
55 solutions to reduce the energy penalty: (1) improving the performance of PCC process, or (2) retrofitting  
56 the steam cycle of power plant with comprehensive heat integrations with PCC process.

57

58 The absorption process has been extensively researched to decrease its reboiler duty. Freguia and  
59 Rochelle [17] performed sensitivity analyses on process variables to find operating conditions at low  
60 energy requirement. Moullec et al. [18] and Babatunde et al. [19] evaluated various process modifications  
61 through modelling and simulation. A variety of single solvents and blended solvents are studied and compared  
62 to find advanced solvents possessing good performance and low price [20-22]. These processes are run in the  
63 scale of pilot plant, however, another difficulty of commercial application of PCC technology in CFPP is to  
64 evaluate the performance of PCC plants in industrial scale. Lawal et al. [16] scaled up the process according to  
65 chemical engineering principles to match a specific CFPP.

66 Several other researchers focus on the thermal efficiency of CFPPs to improve the steam conditions in boiler.  
67 Weitzel et al. [24] improved the overall CFPP thermal efficiency by 6% through adopting 700 °C technology in  
68 steam generator instead of 600 °C technology. However, the steam conditions are related to the materials in  
69 steam generator, critical steam piping and steam turbine. Thus this method is infeasible for retrofits of existing  
70 CFPPs. One main strategy is recovering the waste heat of PCC plant to heat circulating water, which contributes  
71 to a reduction of steam extraction for solvent regeneration. Hanak et al. [3] reduced the efficiency penalty by  
72 0.43% through heat exchanger network (HEN) analysis. In the study of Gibbins and Crane [25], extracted steam  
73 is desuperheated through exchanging heat with part of the reboiler condensate, and waste heat from CO<sub>2</sub> capture  
74 and compression process is recovered by heating circulating water, decreasing the efficiency penalty by 2.9%  
75 for MEA and by 2.5% for KS-2. Besides, Lucquiaud and Gibbins [26] compared three capture ready steam  
76 turbine options (clutched LP turbine, throttled LP turbine and Floating IP/LP crossover pressure), revealing that  
77 the case with clutched LP turbine presented lowest efficiency penalty.

78 Based on above research, this paper focuses on the integration of steam cycle and PCC plant,  
79 comprehensively considering heat exchanger network analysis, utilization of the superheat of extracted

---

80 steam, capture ready steam turbine options and steam-extraction locations. To do this, the steam cycle of a  
81 600MW<sub>e</sub> supercritical CFPP was modelled and simulated, as well as the CO<sub>2</sub> capture and compression  
82 process. The CO<sub>2</sub> capture process is scaled up to match the capacity of the 600MW<sub>e</sub> supercritical CFPP.  
83 Furthermore, eight cases were simulated and compared regarding the energy efficiency improvement.

84 Two novelties can be claimed for this paper: 1) detailed study on scale-up of PCC process to match the  
85 flue gas flowrate of a specific 600 MW<sub>e</sub> supercritical CFPP was performed. 2) comprehensive heat  
86 integration options were studied for two different stream extraction from LP I (at 3.64 bar) and IP-LP  
87 crossover (at 9.1 bar) respectively for solvent regeneration. Compared with previous studies such as Lawal  
88 et al. (2012) [16], this study considered not only how to extract steam from steam turbine in power plant  
89 for PCC reboiler, but also heat integrations between PCC, CO<sub>2</sub> compressors and CFPP. More important is  
90 that these possibilities have been combined in the case study.

91

## 92 **2. Model development**

### 93 *2.1. Model development of Supercritical CFPP*

94

95 Selected as the reference power plant was a 600 MW<sub>e</sub> supercritical CFPP (24.2 MPa/571°C/569°C) in  
96 China (Figure1), in which approximately 1677.5t/h of high-pressure steam generated in the steam  
97 generator passes through HP, IP, and LP turbines successively for electric power generation. In this power  
98 plant, the exhausted steam is next condensed to water in the condenser at pressure of 0.0588bar, and eight-  
99 stage steam (HP I & HP II; IP I & IP II; LP I, LP II, LP III & LP IV) is drawn off to heat the circulating  
100 water (see Table 1). The first three-stage steam extraction is for HP feedwater heaters; the fourth-stage  
101 steam extraction is for deaerator; and the last four-stage steam extraction is for LP condensate heaters. In  
102 addition, fuel combustion produces a large amount of flue gas. Before entering the CO<sub>2</sub> capture process,  
103 flue gas is often treated with a series of chemical processes and scrubbers to remove particulate matter  
104 and sulphur dioxide.

105 This supercritical CFPP is modelled in Aspen Plus<sup>®</sup> as base case to explore the influence of PCC  
106 integration. The *STEAMNBS* property method is used to properly evaluate the steam process. All turbines  
107 are simulated using *Compr* blocks set as isentropic turbines, and circulating water heaters are modelled as  
108 *HeatX* blocks [23]. The boiler is replaced as a *HeatX* block to simplify the process. The overall  
109 performance is shown in Table 2.

110

### 111 *2.2. Model development and scale-up of PCC process*

#### 112 *2.2.1. PCC process description*

113 Figure 2 shows a typical CO<sub>2</sub> chemical absorption process. CO<sub>2</sub> from flue gas is chemically absorbed by  
114 an MEA solution in the absorber column and then released from the top of the regenerator column with  
115 high concentration. In this study, a closed-loop rate-based CO<sub>2</sub> absorption model is developed in Aspen  
116 Plus<sup>®</sup> and validated using the data from a pilot plant at University of Texas, Austin [27, 28]. All  
117 parameters in the model and validation process are stated by Canepa, et al [23]. In the pilot plant, both the

---

118 absorber and regenerator column are 0.427m in diameter and packed with two sections of 3.05m packing.  
119 The absorber is operated at atmospheric pressure with a random metal packing, IMTP no.40, while the  
120 regenerator is operated at a pressure of 1.7 bar and filled with a structured packing, Flexi Pac1Y.

121

### 122 2.2.2. Model scale-up

123 To match the capacity of a 600 MW<sub>e</sub> supercritical CFPP, the CO<sub>2</sub> capture plant model has been scaled  
124 up based on chemical engineering principles. As an initial input of Aspen Plus<sup>®</sup> model, a first-guess  
125 diameter is required for the absorber and the regenerator. One engineering practice is to calculate the  
126 column diameter from the maximum flooding vapour velocity which could be estimated by empirical  
127 correlation equations and figures. In this study, a generalised pressure drop correlation figure (see Figure  
128 11.46. in [29]) adapted from a figure by the Norton Co. was used. The abscissa and ordinate are presented  
129 in Equation (1) and Equation (2) respectively [29].

130

$$131 \quad F_{LV} = \frac{L_w^*}{V_w^*} \sqrt{\frac{\rho_V}{\rho_L}} \quad (1)$$

$$132 \quad K_4 = \frac{13.1(V_w^*)^2 \cdot F_p \cdot (\mu_L / \rho_L)^{0.1}}{\rho_V(\rho_L - \rho_V)} \quad (2)$$

133  $F_{LV}$  is a flow parameter which is related to L/G ratio;  $K_4$  is a modified load which is evaluated from Figure  
134 11.46. in [29] according to the value of  $F_{LV}$  and assumed pressure drop.  $F_p$  is a packing factor. Based on  
135 this,  $V_w^*$  (vapour mass flow rate per unit cross-sectional area) is calculated, then the total cross-sectional  
136 area can be obtained given the flue gas flow rate. This methodology has also been applied in numerous  
137 similar literatures [3, 16, 23].

138 Flooding and minimum liquid load are two primary limitations for the operating region of packed  
139 columns. Flooding defines the upper operating line of packed column. The minimum liquid load is set to  
140 ensure that the entire packing surface is wetted [16, 30]. In order to achieve good liquid and gas  
141 distribution, pressure drop between 15 and 50 mmH<sub>2</sub>O per meter packing for absorber and regenerator  
142 columns was recommended [29]. In this paper, pressure drop of 42 mmH<sub>2</sub>O per meter packing is selected  
143 for the scale-up [3]. Here one important thing should be noticed that the design of the column internals  
144 such as gas/liquid distributors and re-distributors is crucial to ensure good gas and liquid distribution inside  
145 the absorber and regenerator in such large diameters.

146 The boundary conditions data can be seen in Table 3. A first-guess diameter of the absorber and  
147 regenerator can be calculated using the above method. Starting from this, these parameters will be  
148 improved in the development of the closed-loop CO<sub>2</sub> absorption model in Aspen Plus<sup>®</sup>. In the simulation  
149 of the closed-loop capture plant, lean loading (mol CO<sub>2</sub>/mol MEA) is an important parameter related to  
150 reboiler duty. The change of reboiler duty at different lean loadings is presented in Figure 3; here it can be  
151 seen that the reboiler duty first decreases as lean loading increases, and then it increases with the increase  
152 of lean loading. Minimum reboiler duty is attained when lean loading is 0.23 mol CO<sub>2</sub>/mol MEA.

---

The relationship of different numbered columns and diameters is given in Figures 4 and 5. Considering structural limitations, it is better to keep the column diameter less than 12.2m—thus, for the absorber, at least three columns with diameters of 11.66m are needed [16, 31] whilst a two-column regenerator with a diameter of 10.78m is selected. The overall performance of the capture plant with improved parameters is shown in Tables 4 and 5.

### 2.3. Simulation of compression process

After the CO<sub>2</sub> captured from the power plant, it will be pressurized at a pressure as high as 110 -150 bar for pipeline transport and geologic sequestration [32, 33]. Thus a compression train is needed. In this study, CO<sub>2</sub> is pressurized to 90 bar by a four-stage compressor and then pressurized to 110bar by a pump. Between two adjacent stages of the compressor, an intercooler cools the stream. A flash tank is set after the intercooler of the first stage and second stage to draw off liquid water (Figure 6). In the simulation, isentropic compression model is selected with 90% isentropic efficiency [18]. And the pressure drop of intercoolers is assumed as 2% [34]. Simulation results are given in Table 6. There are four hot streams that need to be cooled in the process, and the heat can be integrated into the steam cycle.

## 3. Integration of CFPP with PCC and compression process

A large amount of steam is drawn off from steam cycle to heat the reboiler because of the huge energy required for solvent regeneration, as shown in Figure 7. In this way, all of the low-pressure condensate heaters are removed, and a throttling valve (V1 in Figure 7) is added at the steam extraction location to ensure the plant's stability [35]. The solvent regeneration temperature in the reboiler of the capture plant is 120°C, meaning that hot steam used to heat the reboiler should be 130°C with 10°C mean temperature difference—that is to say that steam of 2.7 bar is required for solvent regeneration. However, the steam extraction point is not casual; Table 1 details the eight stages of steam extraction in the steam cycle. Consequently, the steam drawn off for solvent regeneration is usually decompressed to 2.7 bar by a throttling valve V2 and cooled down to just above saturated temperature through transferring heat with circulating water in H4. The power plant without PCC process has been simulated as the Base Case in Section 2.2. In this section, this study focuses on the effect of PCC plant integration on power plant performance.

### 3.1. Steam extraction from LP I (i.e. 3.64 bar)

#### 3.1.1. Considerations

For the location selection of steam extraction for solvent regeneration, LP I (at 3.64 bar) is appropriate because it is closest to 2.7 bar as seen in Table 1. After the steam is drawn from LP I, the steam is decompressed to 2.7 bar and then cooled to its saturated state before entering the reboiler in PCC process.

In the steam cycle, thermal energy is needed to heat circulating water. In general, this energy is provided by eight-stage steam extraction for a standalone CFPP. Once CFPP is integrated with CO<sub>2</sub> capture and

---

191 compression process, energy saving could be achieved by coupling the hot streams of capture and  
192 compression process with the steam cycle to heat circulating water. The properties of hot streams are  
193 presented in Table 7. The stream named 'CO<sub>2</sub> cooling' is from the last compressor and required to be  
194 condensed to enter a pump. It should be noted that the heat load of the stream shown here does not involve  
195 the heat of condensation because the condensation temperature is too low to be utilized. The highest  
196 temperature of hot streams in Table 7 is 167°C whilst circulating water is heated from 34°C to 175.9°C in  
197 LP condensate heaters and then is heated from 175.9°C to 272°C in HP feedwater heaters. Therefore, only  
198 circulating water in the low-temperature section can be heated by waste heat from CO<sub>2</sub> capture and  
199 compression process.

200

201 Moreover, a great amount of steam is drawn off for solvent regeneration; thus a throttling valve is  
202 generally added to keep the stability, resulting in a throttling loss. On the other hand, there are usually  
203 several sets of LP cylinders in the plant to avoid the turbine blade becoming too long when steam  
204 expanding in power generation process. Consequently, if part of the LP turbine is taken out of service, the  
205 rest LP turbine can work at conditions close to normal operating state; accordingly, the throttling loss is  
206 avoided.

207

### 208 3.1.2. Case studies

209 For the scenario of steam extraction from LP I stream (3.64 bar) for solvent regeneration, three cases are  
210 set up to study the effect of utilizing waste heat and taking part of the LP turbine out of service in below:

211 Case 1A: Basic integration of PCC into supercritical CFPP with steam extraction from LP I for PCC  
212 reboiler.

213 Case 2A: Utilizing waste heat from the PCC and CO<sub>2</sub> compression process for feedwater pre-heating in  
214 CFPP & steam extraction from LP I in CFPP for PCC reboiler.

215 Case 3A: Taking part of LP cylinders out of service & Utilizing waste heat from the PCC and CO<sub>2</sub>  
216 compression process for feedwater pre-heating in CFPP & steam extraction from LP I in CFPP for PCC  
217 reboiler.

218 These three cases are set progressively, and the flow chart of case 3A is shown in Figure 8. In the  
219 process of waste heat utilization,  $\Delta T$  for heat transfer is set to 10°C. The circulating water is heated to 74°C  
220 by the condenser of regenerator first, then it is divided into four parts and exchange heat with the four  
221 intercoolers of compression process respectively, as a result, the four streams are heated to 138°C, 125°C,  
222 131°C and 157°C respectively, and the average temperature is 139°C. So that the effect of PCC integration  
223 can be investigated, the performance of the cases is presented as net power output, generating efficiency  
224 and CO<sub>2</sub> emissions, and compared with the base case described in section 2.2. Simulation results  
225 comparison between these three cases and the base case are given in table 8. Generally introduction of the  
226 CO<sub>2</sub> capture process results in a large efficiency penalty in the supercritical CFPP. In Case 1A, the  
227 efficiency penalty is 12.29% points and equals a decrease of 29.5% in the economic benefits of the power  
228 plant. Waste heat is recovered in Case 2A, which makes an improvement of 0.54% points in generating

---

229 efficiency. This is because waste heat utilization decreases the flow rate of steam extraction for circulating  
230 water heating. Furthermore, more than half of the LP steam is drawn off, and a throttling valve is added to  
231 ensure the power plant stability. However, if half of the LP turbine is taken out of service, the other half  
232 can still work in approximately normal condition; therefore, the throttling loss is avoided. The power plant  
233 performance is shown in case 3A in which generating efficiency is improved by 0.9% after taking half of  
234 the LP turbine out of service. Moreover, for new power plants, the capacity of every LP cylinder can be  
235 designed according to the flow rate of steam extraction, which allows the corresponding LP cylinder to  
236 shut down when integrating with PCC.

237

### 238 *3.2. Steam extraction from IP-LP crossover (i.e. 9.1 bar)*

#### 239 *3.2.1. Considerations*

240 The overall performance of the power plant with steam extraction from LP I (i.e. 3.64 bar) was studied  
241 in Section 3.1. Theoretically it is feasible to draw steam from any stage of steam turbine with pressure  
242 higher than 2.7bar for solvent regeneration. However, it is not economical to draw steam when steam  
243 pressure is too high considering the large throttling loss. As a typical case, we study steam extraction from  
244 IP-LP crossover with steam pressure at 9.1 bar. The consideration of setting up Cases 1B, 2B and 3B is  
245 similar to what has been analysed in Section 3.1.

246

#### 247 *3.2.2. Case studies*

248 Three cases are developed to compare the performance of power plant with 9.1 bar steam extraction:

249 Case 1B: Basic integration of PCC into supercritical CFPP with steam extraction from IP-LP crossover  
250 for PCC reboiler.

251 Case 2B: Utilizing waste heat from the PCC and CO<sub>2</sub> compression process for feedwater pre-heating in  
252 CFPP & steam extraction from IP-LP crossover in CFPP for PCC reboiler.

253 Case 3B: Taking part of LP cylinders out of service & Utilizing waste heat from the PCC and CO<sub>2</sub>  
254 compression process for feedwater pre-heating in CFPP & steam extraction from IP-LP crossover in CFPP  
255 for PCC reboiler.

256 In Case 2B and Case 3B, the temperature of the steam, which is freshly decompressed from 9.1 bar  
257 steam, is too high to be cooled down to the saturated temperature by preheated circulating water. For such  
258 a situation, part of the steam cooled down in the reboiler is returned back to mix with high-temperature  
259 steam to effect the appropriate temperature, as shown in figure 9. In this way, less steam is drawn off and  
260 more is used to generate electricity. Meanwhile, more condensate is produced from the condenser,  
261 resulting in that waste heat from PCC plant is not able to improve the circulating water to the same  
262 temperature in Case 3A. In the heat exchanger network, circulating water is heated to 74°C first, then it is  
263 divided into four streams which are heated to 133°C, 115°C, 127°C and 152°C respectively, the average  
264 temperature is 133°C. The overall performance of these cases is presented in table 9.

265 From results (for steam extraction at IP-LP crossover) shown in Table 9, the net efficiency penalty in  
266 Cases 1B, 2B and 3B are 14.9%, 14.04% and 13.0% respectively. However from results (for steam

---

267 extraction at LP I) shown in Table 8, the net efficiency penalty in Cases 1A, 2A and 3A are 12.29%, 11.75%  
268 and 10.85% respectively. By comparison, steam extraction at lower pressure is more economical. This can  
269 be explained theoretically that the throttling loss of decompressing higher pressure steam (9.1 bar) to 2.7  
270 bar is more serious. On the other hand, the reduction of efficiency penalty from Case 1B to Case 3B (1.9%)  
271 is lightly higher than it from Case 1A to Case 3A (1.44%). This is because the 9.1 bar steam saved in Case  
272 3B due to heat integration is higher grade stream, resulting in a higher power output increment.

273

### 274 *3.3. Auxiliary turbine*

275

276 From Section 3.1 and Section 3.2, the net power output is improved through utilizing waste heat and  
277 taking half of LP turbine out of service. However, the throttling valve V2 is still causing energy loss,  
278 especially in Case 3B. In this section, the addition of an auxiliary turbine to decompress the steam  
279 extracted from IP-LP crossover at 9.1 bar is considered. The throttling valve V2 is no longer necessary. As  
280 this case is a further extension of Case 3B, this case is called Case 4B:

281 Case 4B: adding an auxiliary turbine (see Figure 10) to decompress the extraction steam & taking part of  
282 LP cylinders out of service & utilizing waste heat from the PCC and CO<sub>2</sub> compression process for  
283 feedwater pre-heating in CFPP & steam extraction from IP-LP crossover in CFPP for PCC reboiler.

284 In Case 4B, the steam decompressed by the auxiliary turbine possesses less superheat to heat circulating  
285 water and reboiler condensate. Thus more 9.1 bar steam than that in Case 3B is extracted to match the  
286 reboiler duty, resulting in less condensate from condenser. In this way, circulating water from condenser is  
287 able to be heated to higher temperature than that in Case 4B through waste heat recovery. Specifically, the  
288 circulating water from condenser is heated to 74°C first, then it is divided into four streams which are  
289 heated to 138°C, 125°C, 131°C and 157°C respectively. The average temperature is 139°C. The  
290 performance can be seen in Table 10. The net efficiency penalty in Case 4B is 9.75%, this result  
291 demonstrates a substantial improvement of a 4% increment compared with Case 3B. Thus it can be seen  
292 that the throttling loss in Case 3B is huge. The net efficiency penalty in this case is 9.75%, 1.1% points less  
293 than it in Case 3A. Among all cases presented, Case 4B represents the best performance.

294

## 295 **4. Conclusions**

296

297 In this study, a steady state model for 600 MW<sub>e</sub> supercritical CFPP was developed, and seven cases were  
298 studied to investigate the effect of integration with PCC process and CO<sub>2</sub> compression process. Generating  
299 efficiency for the reference case is 41.6%. It reduced to 29.31% when more than half of the steam was  
300 extracted from LP I (at 3.64 bar) for solvent regeneration. Two methods, utilization of waste heat from  
301 PCC process and CO<sub>2</sub> compression process and taking half of LP turbine out of service, were adopted to  
302 decrease the efficiency penalty, which improved the generating efficiency to 30.75%. Similar study was  
303 performed in the cases of extracting steam from IP-LP crossover at 9.1 bar. The generating efficiency  
304 reduced to 26.7% in the basic integration, and improved to 28.6% through adopting the two methods.  
305 Extracting steam from IP-LP crossover at 9.1 bar caused more serious efficiency penalty due to the higher



---

306 throttling loss. However, an auxiliary turbine was added to decompress the 9.1 bar steam, which  
307 contributed to a reduction of 3.25% in efficiency penalty. In this way, net generating efficiency is 31.85%  
308 and the efficiency penalty is reduced to 9.75%. According to the results, comprehensive heat integration  
309 modifications can effectively reduce the energy penalty when the CFPP is integrated with PCC and CO<sub>2</sub>  
310 compression process.

## 311 **Acknowledgement**

314 The authors would like to acknowledge the financial support from the National Natural Science  
315 Foundation of China (key project No. 51134017), EU FP7 Marie Curie International Research Staff  
316 Exchange Scheme (Ref: PIRSES-GA-2013-612230) and State Key Laboratory of Chemical Engineering of  
317 China (SKL-ChE-12Z01).

## 319 **References**

- 320 [1] IPCC. Climate change 2014: mitigation of climate change: contribution of working group III to the fifth  
321 assessment report of the intergovernmental panel on climate change. Cambridge, United Kingdom and  
322 New York, NY, USA: Cambridge University Press; 2014.
- 323 [2] IPCC. Managing the risks of extreme events and disasters to advance climate change adaptation.  
324 Cambridge, United Kingdom and New York, NY, USA: Cambridge University Press; 2012.
- 325 [3] Hanak DP, Biliyok C, Yeung H, Bialecki R. Heat integration and exergy analysis for a supercritical high-ash  
326 coal-fired power plant integrated with a post-combustion carbon capture process. *Fuel* 2014; 134: 126-  
327 139.
- 328 [4] IEA. Energy technology perspectives 2010: scenarios & strategies to 2050. Paris, France: IEA Publications;  
329 2010.
- 330 [5] IEA. Technology roadmap: carbon capture and storage. Paris, France: IEA Publications; 2013.
- 331 [6] IEA. Tracking clean energy progress 2013: IEA input to the clean energy ministerial. Paris. France: IEA  
332 Publications; 2013.
- 333 [7] Goto K, Yogo K, Higashii T. A review of efficiency penalty in a coal-fired power plant with post-combustion  
334 CO<sub>2</sub> capture. *Applied Energy* 2013; 111: 710-720.
- 335 [8] Wang M, Lawal A, Stephenson P, et al. Post-combustion CO<sub>2</sub> capture with chemical absorption: A state-of-  
336 the-art review. *Chemical Engineering Research and Design* 2011; 89:1609-1624.
- 337 [9] Alie C, Backham L, Croiset E, Douglas PL. Simulation of CO<sub>2</sub> capture using MEA scrubbing: a flowsheet  
338 decomposition method. *Energy Conversion and Management* 2005; 46: 475-487.
- 339 [10] Kanniche M, Gros-Bonnivard R, Jaud P, et al. Pre-combustion, post-combustion and oxy-combustion in  
340 thermal power plant for CO<sub>2</sub> capture. *Applied Thermal Engineering* 2010; 30: 53-62.
- 341 [11] Rao AB, Rubin ES. A technical, economic, and environmental assessment of amine-based CO<sub>2</sub> capture  
342 technology for power plant greenhouse gas control. *Environmental science & technology* 2002; 36: 4467-  
343 4475.
- 344 [12] Singh d, Croiset E, Douglas PL, Douglas MA. Techno-economic study of CO<sub>2</sub> capture from an existing coal-  
345 fired power plant: MEA scrubbing vs. O<sub>2</sub>/CO<sub>2</sub> recycle combustion. *Energy Conversion and Management*  
346 2003; 44: 3073-3091.
- 347 [13] Lawal A, Wang M, Stephenson P, Yeung H. Dynamic modelling of CO<sub>2</sub> absorption for post combustion  
348 capture in coal-fired power plants. *Fuel* 2009; 88: 2455-2462.
- 349 [14] Abu-Zahra MRM, Schneiders LHJ, Niederer JPM, et al. CO<sub>2</sub> capture from power plants: Part I. A parametric  
350 study of the technical performance based on monoethanolamine. *International Journal of Greenhouse*  
351 *Gas Control* 2007; 1: 37-46.
- 352 [15] Davison J. Performance and costs of power plants with capture and storage of CO<sub>2</sub>. *Energy* 2007; 32:  
353 1163-1176.
- 354 [16] Lawal A, Wang M, Stephenson P, Obi O. Demonstrating full-scale post-combustion CO<sub>2</sub> capture for coal-  
355 fired power plants through dynamic modelling and simulation. *Fuel* 2012; 101: 115-128.
- 356 [17] Freguia S, Rochelle GT. Modeling of CO<sub>2</sub> capture by aqueous monoethanolamine. *AIChE Journal* 2003; 49:

- 
- 357 1676-1686.
- 358 [18] Moullec YL, Kanniche M. Screening of flowsheet modifications for an efficient monoethanolamine (MEA)  
359 based post-combustion CO<sub>2</sub> capture. *International Journal of Greenhouse Gas Control* 2011; 5: 727-740.
- 360 [19] Oyekan B A, Rochelle G T. Alternative stripper configurations for CO<sub>2</sub> capture by aqueous amines. *AIChE*  
361 *Journal* 2007, 53(12): 3144-3154.
- 362 [20] Freeman S A, Dugas R, Van Wagener D H, Nguyen T, Rochelle G T. Carbon dioxide capture with  
363 concentrated, aqueous piperazine. *Int J Greenhouse Gas Control* 2010; 4: 119–124
- 364 [21] Aroonwilas A, Veawab A. Integration of CO<sub>2</sub> capture unit using single- and blended-amines into  
365 supercritical coal-fired power plants: implications for emission and energy management. *Int J Greenhouse*  
366 *Gas Control* 2007; 1: 143–150.
- 367 [22] Conway W, Bruggink S, Beyad Y, et al. CO<sub>2</sub> absorption into aqueous amine blended solutions containing  
368 monoethanolamine (MEA), N, N-dimethylethanolamine (DMEA), N, N-diethylethanolamine (DEEA) and 2-  
369 amino-2-methyl-1-propanol (AMP) for post combustion capture processes. *Chemical Engineering Science*  
370 2014; 126: 446-454.
- 371 [23] Canepa R, Wang M, Biliyok C, Satta A. Thermodynamic analysis of combined cycle gas turbine power plant  
372 with post-combustion CO<sub>2</sub> capture and exhaust gas recirculation. *Proceedings of the Institution of*  
373 *Mechanical Engineers* 2013; 227: 89-105.
- 374 [24] Weitzel P S, Tanzosh J M, Boring B, et al. Advanced Ultra-Supercritical Power Plant (700 to 760C) Design  
375 for Indian Coal. *Power-Gen Asia* 2012, Bangkok, Thailand.
- 376 [25] Gibbins J R, Crane R I. Scope for reductions in the cost of CO<sub>2</sub> capture using flue gas scrubbing with amine  
377 solvents. *Proceedings of the Institution of Mechanical Engineers, Part A: Journal of Power and Energy*  
378 2004; 218(4): 231-239.
- 379 [26] Lucquiaud M, Gibbins J. Retrofitting CO<sub>2</sub> capture ready fossil plants with post-combustion capture. Part 1:  
380 requirements for supercritical pulverized coal plants using solvent-based flue gas scrubbing. *Proceedings*  
381 *of the Institution of Mechanical Engineers, Part A: Journal of Power and Energy* 2009; 223(3): 213-226.
- 382 [27] Dugas RE. Pilot plant study of carbon dioxide capture by aqueous monoethanolamine (MSc Thesis), The  
383 University of Texas, Austin, USA, 2006.
- 384 [28] Zhang Y, Chen H, Chen C C, et al. Rate-based process modeling study of CO<sub>2</sub> capture with aqueous  
385 monoethanolamine solution. *Industrial & engineering chemistry research* 2009; 48(20): 9233-9246.
- 386 [29] Towler G, Sinnott RK. *Chemical engineering design: principles, practice, and economics of plant and*  
387 *process design*. 2nd ed. Oxford, UK: Elsevier; 2013.
- 388 [30] Stichlmair FJ, Johann G. *Distillation: principles and practices*. New York, USA: Wiley-VCH; 1998.
- 389 [31] Ramezan M, Skone T, Nsakala N, et al. Carbon dioxide capture from existing coal-fired power plants.  
390 DOE/NETL-401/110907; NETL: Pittsburgh, PA: 2007.
- 391 [32] Luo X, Mistry K, Okezue C, Wang M, et al. Process Simulation and Analysis for CO<sub>2</sub> Transport Pipeline  
392 Design and Operation - Case Study for the Humber Region in the UK. *Computer Aided Chemical*  
393 *Engineering* 2014; 1633-1638.
- 394 [33] Luo X, Wang M, Oko E, Okezue C. Simulation-based techno-economic evaluation for optimal design of CO<sub>2</sub>  
395 transport pipeline network. *Applied Energy* 2014; 132: 610-620.
- 396 [34] Witkowski A, Rusin A, Majkut M, Rulik S, Stolecka K. Comprehensive analysis of pipeline transportation  
397 systems for CO<sub>2</sub> sequestration. Thermodynamics and safety problems. *Energy Convers Manage* 2013; 76:  
398 665–673.
- 399 [35] Xu G, Yang Y, Ding J, et al. Analysis and optimization of CO<sub>2</sub> capture in an existing coal-fired power plant in  
400 China. *Energy* 2013; 58: 117-127.

---

Table 1. Eight-stage steam extraction

Extraction-stage	HP I	HP II	IP I	IP II	LPI	LP II	LP III	LPIV
Extraction pressure (bar)	61.54	41.48	18.52	9.1	3.64	1.11	0.546	0.175

---

Table 2. Overall performance of the supercritical CFPP without CO<sub>2</sub> capture process

Gross power output (MW <sub>e</sub> )	603.0
Power consumption (MW <sub>e</sub> )	15.5
Net power output (MW <sub>e</sub> )	587.5
Fuel input (MW <sub>th</sub> )	1414
Generating efficiency (%LHV net)	41.6
Flow rate of flue gas (kg/s)	707.8
CO <sub>2</sub> concentration in flue gas ( wt% )	19.54
CO <sub>2</sub> emissions (g/kWh)	841.5

---

---

Table 3. Boundary conditions of PCC process

Flue gas flowrate (kg/s)	707.8
Flue gas CO <sub>2</sub> content (Mole %)	13.09
Flue gas temperature (°C)	44
Solvent MEA content (wt%)	30
Lean solvent flowrate (t/h)	6000
Lean loading (mol CO <sub>2</sub> /mol MEA)	0.23
Capture level	90%
CO <sub>2</sub> stream purity (wt%)	95

---

---

Table 4. Absorber and regenerator design

	Absorber	Regenerator
Pressure drop (mm water/m)	42	42
Column diameter (m)	11.66	10.78
Column number	3	2
Column packing	IMTP no.40	Flexi Pac1Y
Packing height (m)	30	30
Column pressure (bar)	1	1.7

---

Table 5. Overall performance of capture plant

Lean solvent flowrate (t/h)	6995
L/G ratio (mass basis)	2.75
Lean loading (mol CO <sub>2</sub> / mol MEA)	0.23
Rich loading (mol CO <sub>2</sub> / mol MEA)	0.54
Lean Solvent MEA content (wt%)	30.04
CO <sub>2</sub> stream purity (wt%)	94.98
Condenser duty (MW <sub>th</sub> )	40.79
Reboiler duty (MW <sub>th</sub> )	572
Reboiler temperature (°C)	120.46

---

---

Table 6. Performance of CO<sub>2</sub> compression process.

Inlet pressure(bar)	1.7
Outlet pressure (bar)	110
Power consumption(MW <sub>e</sub> )	37.8
CO <sub>2</sub> compression work(kWh/tCO <sub>2</sub> )	84.8
Cold utilities (MW)	84.24

---



Table 7. Property of hot streams

<b>Stream</b>	<b>Stream type</b>	<b>Inlet temperature (°C)</b>	<b>Outlet temperature (°C)</b>	<b>Heat load (MW<sub>th</sub>)</b>
Condenser in Regenerator	Hot	84	59	40.79
CO <sub>2</sub> intercooling 1	Hot	148	51	25.37
CO <sub>2</sub> intercooling 2	Hot	135	54	11.67
CO <sub>2</sub> intercooling 3	Hot	141	73	8.98
CO <sub>2</sub> cooling	Hot	167	36	36.02

Table 8. Thermal performance of Cases with 3.64 bar steam extraction.

<b>Case</b>	<b>Base case</b>	<b>Case 1A</b>	<b>Case 2A</b>	<b>Case3A</b>
<b>Gross power output (MW<sub>e</sub>)</b>	603.0	468.08	475.7	488.35
<b>Pumping work (MW<sub>e</sub>)</b>	15.4	15.8	15.8	15.8
<b>Compression work (MW<sub>e</sub>)</b>	--	37.8	37.8	37.8
<b>Total energy consumption (MW<sub>e</sub>)</b>	15.4	53.6	53.6	53.6
<b>Net power output (MW<sub>e</sub>)</b>	587.6	414.48	422.1	434.75
<b>Fuel input (MW<sub>th</sub>)</b>	1414	1414	1414	1414
<b>Generating efficiency (%)</b>	41.6	29.31	29.85	30.75
<b>Net energy penalty (%)</b>	--	29.46	28.17	26.01
<b>Net efficiency penalty (%)</b>	--	12.29	11.75	10.85
<b>CO<sub>2</sub> emissions (g/kWh)</b>	847.3	120.12	117.95	114.52
<b>CO<sub>2</sub> emission reduction (g/kWh)</b>	--	727.18	729.35	732.78

Table 9. Thermal performance of Cases with steam extraction from IP-LP crossover at 9.1 bar

<b>Case</b>	<b>Base case</b>	<b>Case 1B</b>	<b>Case 2B</b>	<b>Case 3B</b>
<b>Gross power output (MW<sub>e</sub>)</b>	603.0	431.15	443.25	458.03
<b>Pumping work (MW<sub>e</sub>)</b>	15.4	15.8	15.8	15.8
<b>Compression work (MW<sub>e</sub>)</b>	--	37.8	37.8	37.8
<b>Total energy consumption (MW<sub>e</sub>)</b>	15.4	53.6	53.6	53.6
<b>Net power output (MW<sub>e</sub>)</b>	587.6	377.55	389.65	404.43
<b>Fuel input (MW<sub>th</sub>)</b>	1414	1414	1414	1414
<b>Generating efficiency (%)</b>	41.6	26.7	27.56	28.60
<b>Net energy penalty (%)</b>	--	35.75	33.69	31.25
<b>Net efficiency penalty (%)</b>	--	14.9	14.04	13.0
<b>CO<sub>2</sub> emissions (g/kWh)</b>	847.3	131.87	127.77	123.10
<b>CO<sub>2</sub> emission reduction (g/kWh)</b>	--	715.43	719.53	724.20

Table 10. The performance of Case 4B with an auxiliary turbine

<b>Case</b>	<b>Base case</b>	<b>Case 4B</b>
<b>Gross power output (MW<sub>e</sub>)</b>	603.0	503.98
<b>Pumping work (MW<sub>e</sub>)</b>	15.4	15.8
<b>Compression work (MW<sub>e</sub>)</b>	--	37.8
<b>Total energy consumption (MW<sub>e</sub>)</b>	15.4	53.6
<b>Net power output (MW<sub>e</sub>)</b>	587.6	450.38
<b>Fuel input (MW<sub>th</sub>)</b>	1414	1414
<b>Generating efficiency (%)</b>	41.6	31.85
<b>Net energy penalty (%)</b>	--	23.35
<b>Net efficiency penalty (%)</b>	--	9.75
<b>CO<sub>2</sub> emissions (g/kWh)</b>	847.3	110.55
<b>CO<sub>2</sub> emission reduction (g/kWh)</b>	--	736.75

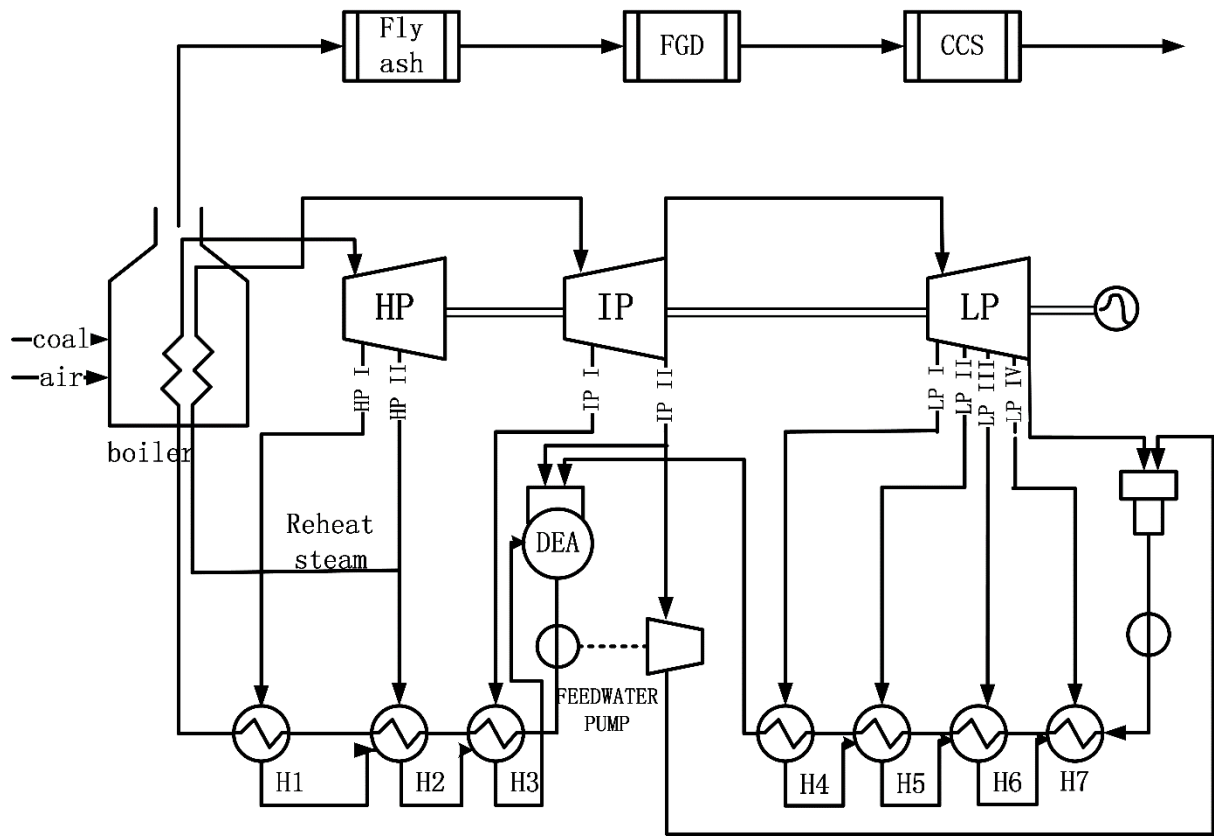


Figure 1. Flow diagram of a 600 MW<sub>e</sub> supercritical CFPP

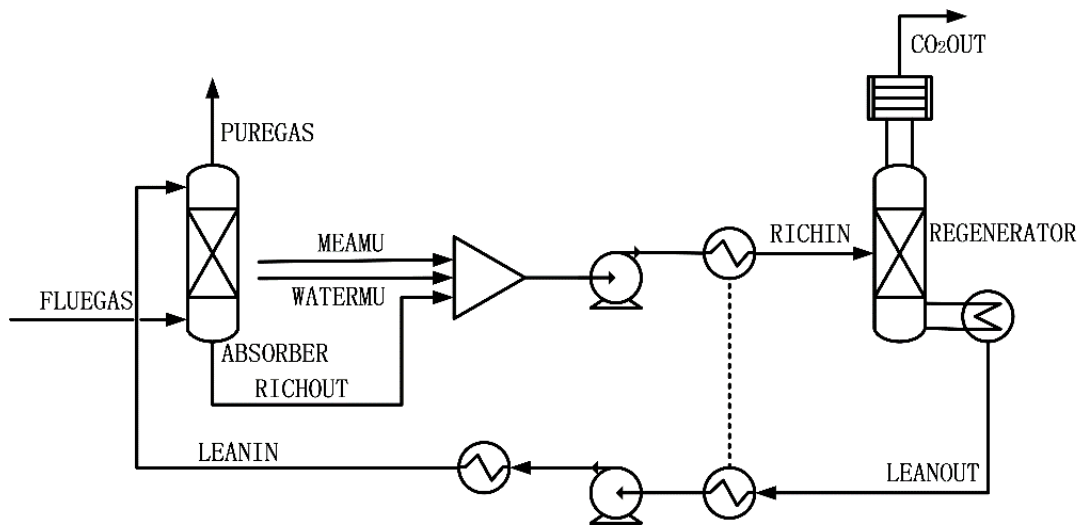


Figure 2. Flowsheet of PCC process

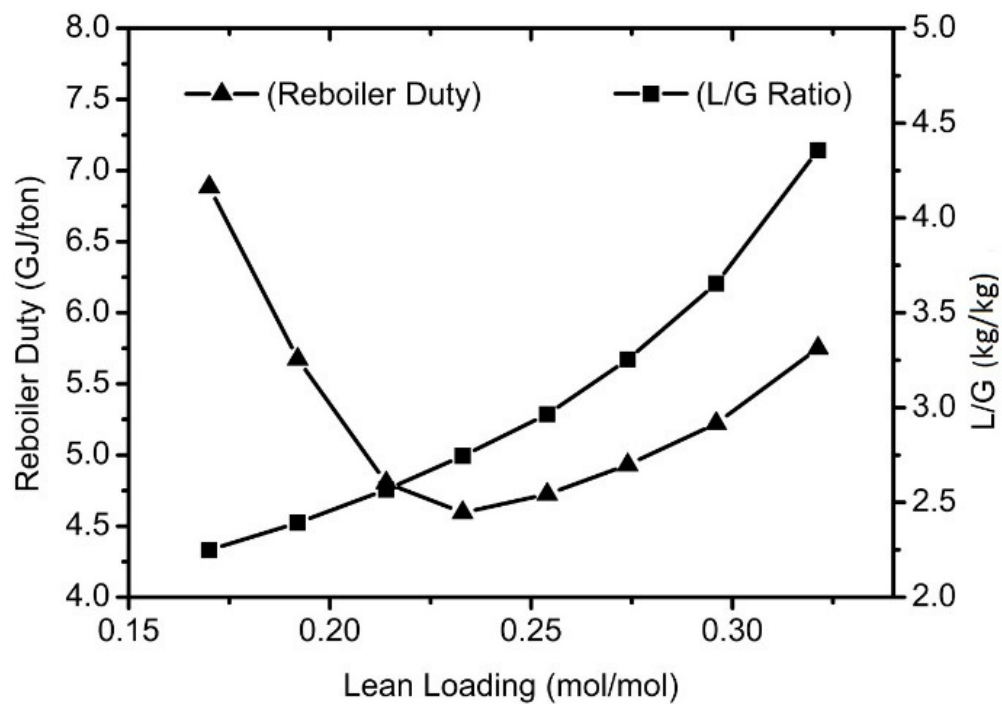


Figure3. Impact of lean loading on reboiler duty and L/G ratio at 90% capture level.

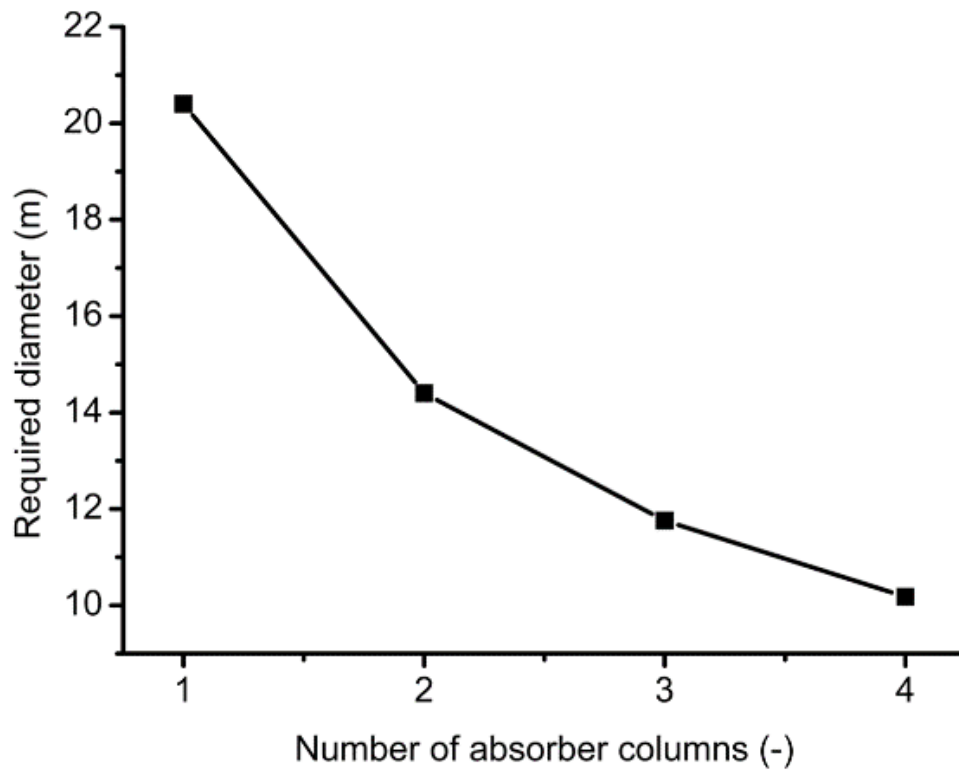


Figure 4. Absorber diameter as function of the number of columns



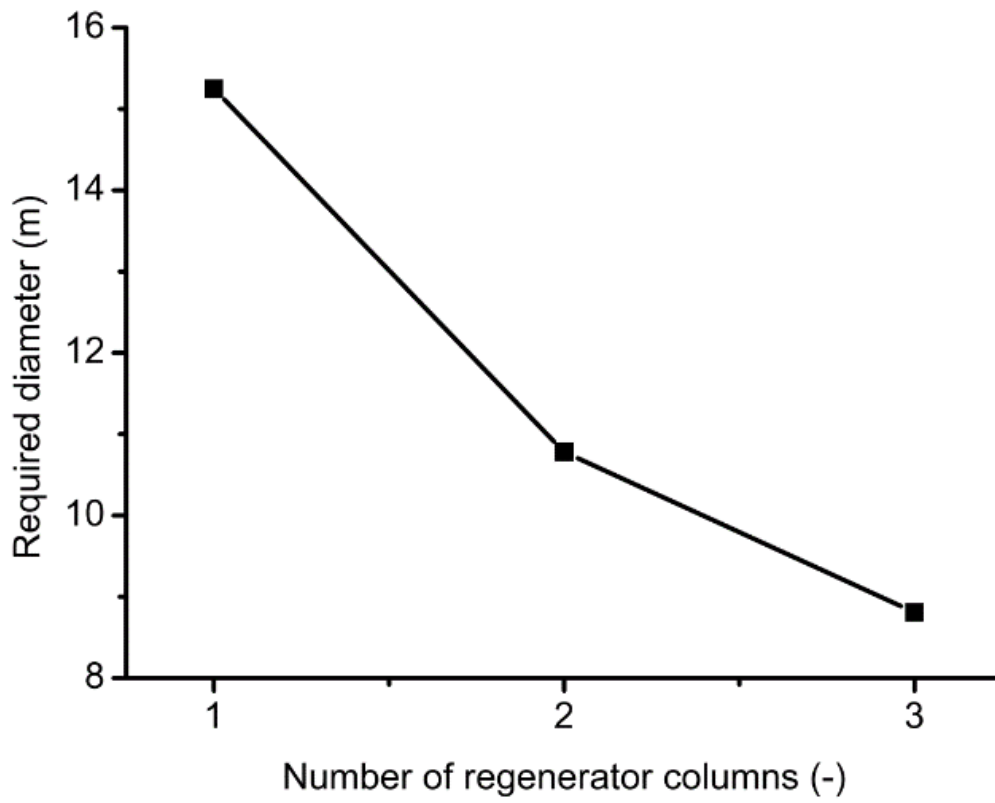


Figure 5. Regenerator diameter as function of the number of columns

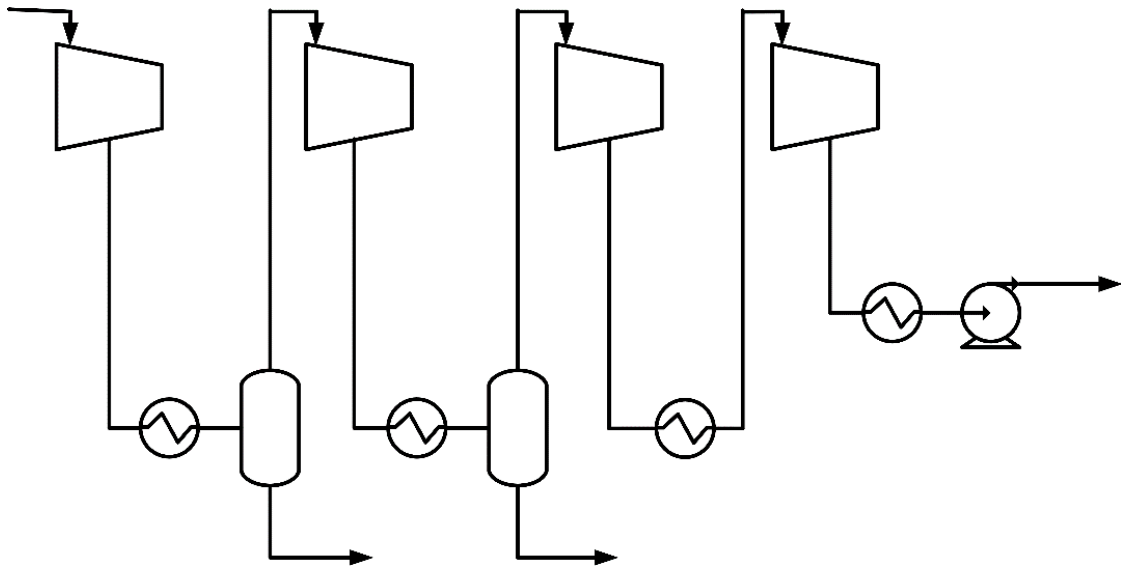


Figure 6. Flowsheet of CO<sub>2</sub> compression process

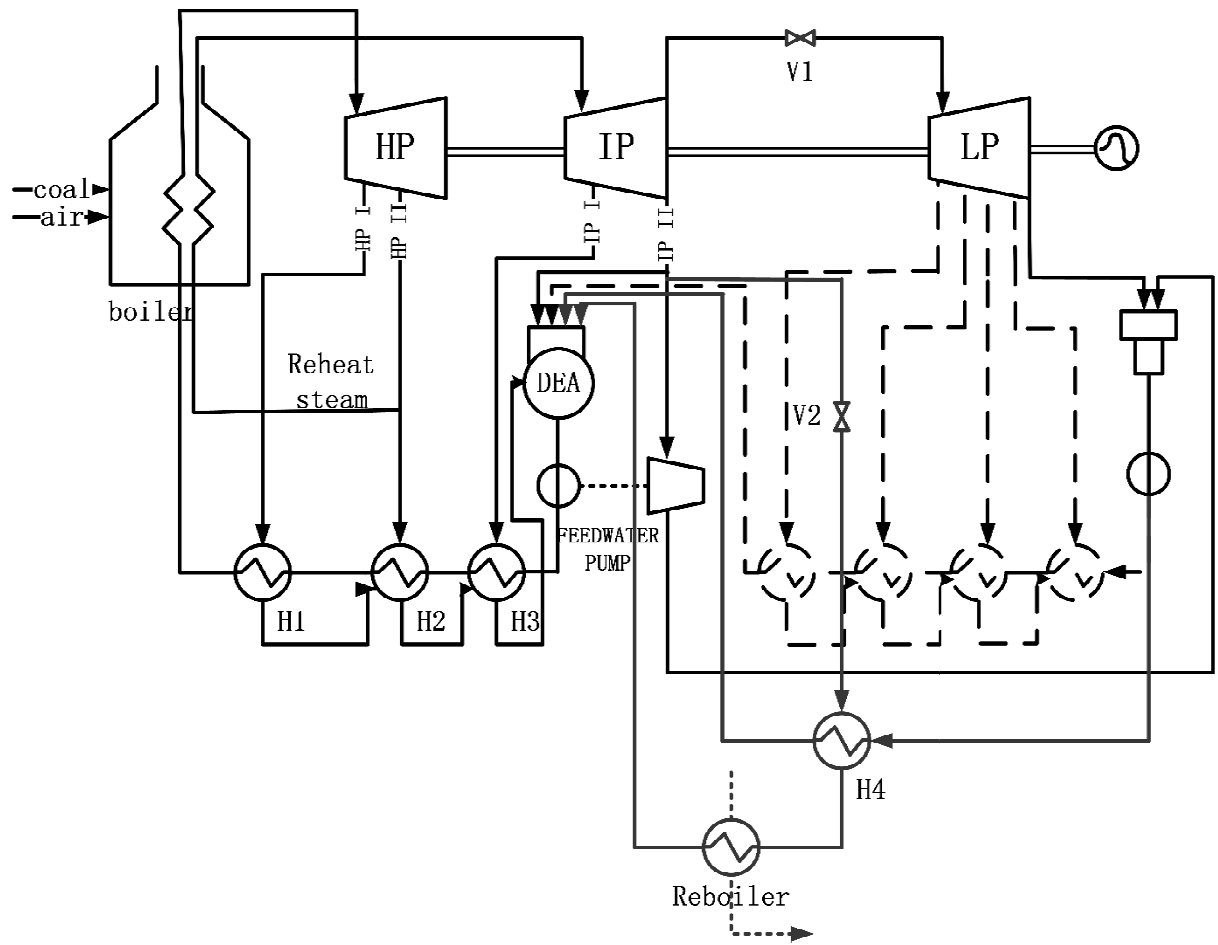


Figure 7. Flow diagram of retrofitted CFCC with CO<sub>2</sub> capture process



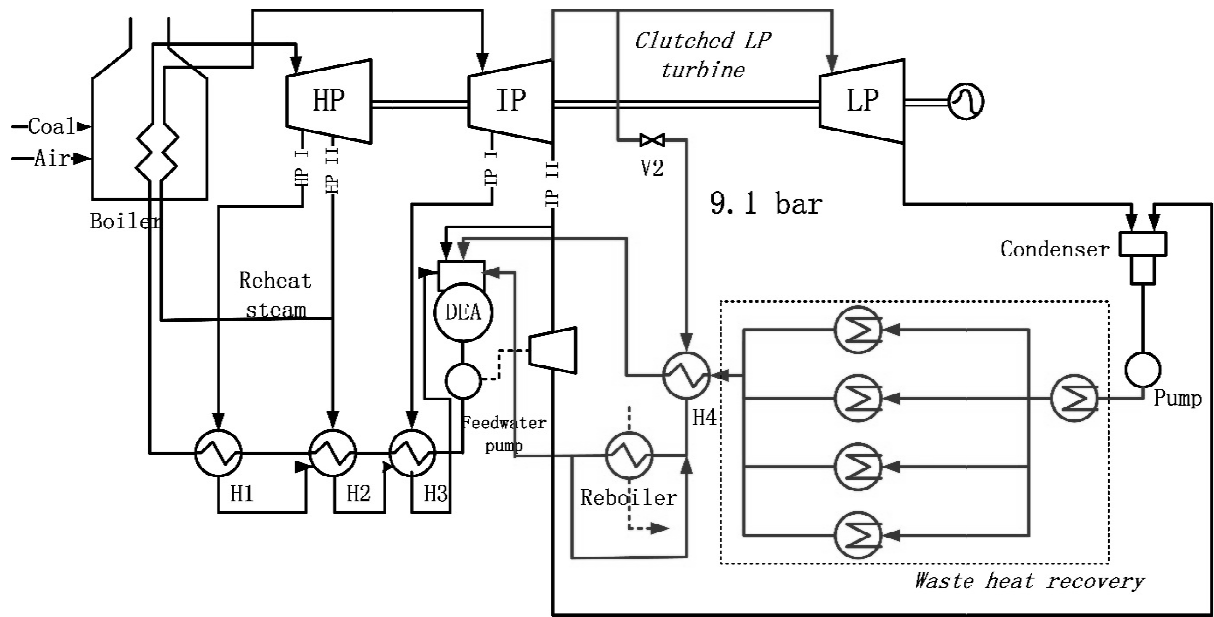


Figure 9. Flow diagram for Case 3B

